Physical Biology

OPEN ACCESS

PAPER

Non-genetic resistance facilitates survival while hindering the evolution of drug resistance due to intraspecific competition

Joshua D Guthrie[1] and Daniel A Charlebois[1,2,*]

[1] Department of Physics, University of Alberta, 11455 Saskatchewan Drive NW, Edmonton, Alberta, Canada
[2] Department of Biological Sciences, University of Alberta, 11455 Saskatchewan Drive NW, Edmonton, Alberta, Canada
[*] Author to whom any correspondence should be addressed.

E-mail: dcharleb@ualberta.ca

RECEIVED
29 July 2022

ACCEPTED FOR PUBLICATION
23 August 2022

PUBLISHED
8 September 2022

Keywords: antimicrobial resistance, deterministic models, population dynamics, stochastic simulations, fluctuating drug conditions, resistance evolution

Abstract

Rising rates of resistance to antimicrobial drugs threaten the effective treatment of infections across the globe. Drug resistance has been established to emerge from non-genetic mechanisms as well as from genetic mechanisms. However, it is still unclear how non-genetic resistance affects the evolution of genetic drug resistance. We develop deterministic and stochastic population models that incorporate resource competition to quantitatively investigate the transition from non-genetic to genetic resistance during the exposure to static and cidal drugs. We find that non-genetic resistance facilitates the survival of cell populations during drug treatment while hindering the development of genetic resistance due to competition between the non-genetically and genetically resistant subpopulations. Non-genetic resistance in the presence of subpopulation competition increases the fixation times of drug resistance mutations, while increasing the probability of mutation before population extinction during cidal drug treatment. Intense intraspecific competition during drug treatment leads to extinction of susceptible and non-genetically resistant subpopulations. Alternating between drug and no drug conditions results in oscillatory population dynamics, increased resistance mutation fixation timescales, and reduced population survival. These findings advance our fundamental understanding of the evolution of resistance and may guide novel treatment strategies for patients with drug-resistant infections.

1. Introduction

Antimicrobial (drug) resistance occurs when bacteria, viruses, fungi, and parasites no longer respond to drug therapy, making infections difficult or impossible to treat, which increases the risk of disease transmission, severe illness, and death [1]. The evolution of genetic drug resistance is known to arise from the natural selection of mutations or resistance genes that provide microbes with the ability to survive and proliferate during treatment [2]. It has also been shown that non-genetic mechanisms promote microbial phenotypic diversification and survival strategies in selective drug environments [3]. Phenotypic heterogeneity has important implications for drug resistance [4, 5], with heritable resistance potentially arising independently of genetic mechanisms [6]. The stochastic or 'noisy' expression of genes [7, 8] introduces phenotypic heterogeneity among genetically identical cells in the same drug environment, which can result in the fractional killing of clonal microbial populations [3, 9], as well as chemotherapy resistance in cancer [10]. This stochasticity is due in part to the inherently random nature of the biochemical reactions involved in the transcription and translation of genetic material, and can lead to the emergence of phenotypically distinct subpopulations within an actively replicating clonal cell population [8, 11]. Another form of non-genetic drug resistance called 'tolerance' occurs in fungi, in which a slow-growing subpopulation of cells (that are genetically identical to susceptible cells) emerges during antifungal drug treatment [12]; related phenomena occur in bacteria [13, 14] and cancer [15].

Non-genetic drug resistance has been proposed to promote the development of genetic drug resistance [4, 5, 10, 12, 16]. This process may be enhanced

by the interaction between non-genetic and genetic mechanisms inside the cell [5]. For instance, promoter mutations can alter the expression noise levels of drug resistance genes [9], genetic network architecture can modulate gene expression noise to enhance drug resistance [17–19], and stress response genes can evolve elevated transcriptional variability through natural selection [20, 21]. Non-genetic mechanisms can facilitate the generation of genetic diversity by increasing the expression of key regulators involved in DNA replication, recombination, or repair [22, 23], as well as by enhancing the adaptive value of beneficial mutations during drug treatment [24] and promoting the fixation of favorable gene expression altering mutations [25]. Non-genetic phenotypic variability can impact cellular populations by providing a link between micro-scale dynamics (such as stochasticity at the molecular level) and macro-scale biological phenomena (including the fate of interacting cell populations) [26]. Such noise in biological systems may facilitate the adaptation to environmental stress by allowing distinct, co-existing cellular states in a population to find the best adaptive solution from multiple starting points [27]. However, there are conflicting views on how phenotypic heterogeneity may facilitate adaptive evolution [28] and the transition from non-genetic to genetic drug resistance remains to be quantified [5, 12].

Fungal pathogens are among the leading causes of infectious disease mortality, which is expected to accelerate due to a variety of factors including climate change [29]. Particularly concerning is the emergence of multidrug resistant yeast pathogens around the globe [30]. Mathematical models and synthetic gene networks (or 'circuits') are being used to experimentally investigate drug resistance in yeast [31]. In particular, synthetic gene circuits have been designed to mimic network motifs that occur naturally, such as positive feedback loops, to study non-genetic resistance in the budding yeast *Saccharomyces cerevisiae* [18, 32, 33]. This positive feedback has been shown to confer yeast cells with a heritable, non-genetically drug-resistant phenotype for up to 283 h before switching back to the drug-susceptible phenotype [32]. These experimental studies reveal important insights into fungal drug resistance and provide parameters for our quantitative models.

Selective pressures during infection can lead to cooperation and competition within microbial communities [34], and these interactions can have implications for disease outcomes [35]. Competition within a microbial community composed of the same species becomes relevant when resources such as nutrients or space become limiting, such as at high population density. Intraspecific competition results from 'exploitation competition', which involves the relatively more efficient use of a limiting resource or from 'interference competition', which results from the production of toxic substances that impair the growth or survival of competitors [36]. Intraspecific competition leads to logistic growth, whereby population growth is exponential when population size and resource competition are low, followed by a progressively reduced growth rate as the population size increases toward the carrying capacity of the micro-environment [37]. Phenotypic heterogeneity can promote interactions among subpopulations as well as the division of labour between individual cells, providing clonal microbial populations with new functionalities [38]. Importantly, the evolutionary effects of intraspecific competition have not been investigated in the context of resource competition between non-genetically and genetically resistant subpopulations in microbial populations undergoing drug treatment.

In this study, we investigate the transition from non-genetic to genetic resistance during static drug (drugs that stop or slow cell growth) and cidal drug (drugs that kill cells) treatment in the presence of resource competition using deterministic and stochastic population models [37]. Overall, we find that non-genetic resistance facilitates the survival of cell populations undergoing drug treatment, while hindering the fixation of genetic mutations due to competition effects between the non-genetically and genetically resistant subpopulations.

2. Methods

2.1. Deterministic population model

The deterministic population model describes changes in cellular subpopulation concentrations over time during drug treatment. Three different subpopulations comprising the total population T are described in this model: a susceptible subpopulation S, a non-genetically resistant subpopulation N, and a genetically resistant subpopulation G. Cells may switch between the S and N subpopulations, and cells in the N subpopulation can mutate into the G subpopulation (figure 1). The mathematical model is described by a set of coupled ordinary differential equations (ODEs):

$$\frac{\mathrm{d}S}{\mathrm{d}t} = Sk'_S + Nr_{S,N} - Sr_{N,S} - S\delta_S \tag{1}$$

$$\frac{\mathrm{d}N}{\mathrm{d}t} = Nk'_N + Sr_{N,S} - Nr_{G,N} - Nr_{S,N} - N\delta_N \tag{2}$$

$$\frac{\mathrm{d}G}{\mathrm{d}t} = Gk'_G + Nr_{G,N} - G\delta_G, \tag{3}$$

where $r_{S,N}$ is the switching rate from N to S, $r_{N,S}$ is the switching rate from S to N, $r_{G,N}$ is the mutation rate from N to G, and δ_S, δ_N, δ_G are the death rates of S, N, and G, respectively. k'_S, k'_N, and k'_G describe the birth rate of each subpopulation in the presence of a drug and resource competition, and are described by equation (6). There is no mutational pathway from S to G, as we are considering drugs that completely

arrest growth and division ($k'_S = 0$) and therefore genetic mutation due to DNA replication errors in the S subpopulation does not occur [39]. Appendix D considers cases where S is allowed to grow ($k'_S \neq 0$), which allows mutation from S to G ($r_{G,S} \neq 0$), and shows that the qualitative trends seen in our main results hold for this scenario. Unless otherwise indicated, we assume that N has partial, temporary resistance (i.e., $0 < \delta_N < \delta_S$) and that genetic mutation provides complete, permanent resistance to the drug. To model static and cidal drug treatments of varying strengths, we respectively varied the birth and death rates in equations (1)–(3).

Summing equations (1)–(3) under the above assumptions yields the following equation for the concentration of the total population:

$$T = S + N + G \tag{4}$$

as well as an equation for the growth rate of the total population:

$$\frac{\mathrm{d}T}{\mathrm{d}t} = Sk'_S + Nk'_N + Gk'_G - S\delta_S - N\delta_N - G\delta_G. \tag{5}$$

Resource competition between the subpopulations was modeled by scaling k_S, k_N, and k_G by a Baranyi-Hill type function, which depends on T and results in logistic growth [37]. The Baranyi model accurately describes the transition from lag-phase to exponential growth that occurs during the adaptation to antimicrobial drugs [37, 40]. For subpopulation i (where, $i \in \{S, N, G\}$), this is given by:

$$k'_i = k_i z(T) = k_i \left(\frac{h^n}{h^n + T^n} \right), \tag{6}$$

where k_i is the maximum birth rate for subpopulation i (which leads to exponential growth in the absence of competition for limited resources), n is the Hill coefficient, and h is the point at which the competition function $z(T)$ is half of its maximum value.

The growth dynamics of S, N, and G were obtained by solving the deterministic model, starting from initial population sizes S_i, N_i, and G_i and numerically integrating equations (1)–(3) over a total time t_{tot} using a time step Δt. This numerical integration was performed using the *ode45* ODE solver, which is based on an explicit Runge–Kutta method, in MATLAB [41]. The fixation time τ_{fix} was used as a quantitative measure of how long it takes for G to become dominant in the population [42] and was defined as the time it takes for G to comprise 95% of the total population.

2.2. Stochastic population model

Next, we developed a stochastic population model corresponding to the deterministic population model to study the effects of non-genetic resistance on the evolution of genetic resistance in low cell number regimes. Low numbers of infectious cells can occur at the onset of infection and during the final stages of drug treatment, and is the regime where stochastic fluctuations are expected to have a significant effect on population dynamics. Accordingly, equations (1)–(3) were translated into the following set of reactions:

$$S \xrightarrow{k'_S} 2S \tag{7}$$

$$N \xrightarrow{k'_N} 2N \tag{8}$$

$$G \xrightarrow{k'_G} 2G \tag{9}$$

$$S \xrightarrow{r_{N,S}} N \tag{10}$$

$$N \xrightarrow{r_{S,N}} S \tag{11}$$

$$N \xrightarrow{r_{G,N}} G \tag{12}$$

$$S \xrightarrow{\delta_S} \oslash \tag{13}$$

$$N \xrightarrow{\delta_N} \oslash \tag{14}$$

$$G \xrightarrow{\delta_G} \oslash \tag{15}$$

equations (7)–(15) were simulated using the Gillespie stochastic simulation algorithm [43, 44].

To quantify the effect of non-genetic drug resistance on the evolution of genetic drug resistance in the stochastic population model, we obtained the first-appearance time (P_τ) and fixation time ($P_{\tau_{\mathrm{fix}}}$) distributions of G. For parameter regimes where population extinction could occur during the cidal drug treatment simulations (i.e., when S and N go extinct before G appears), we determined the effect that the death rate of N had on the probability of G emerging (P_G) before population extinction. This was determined from the number of population extinction events that occurred over a large number of simulations for different values of the death rate for N.

While the deterministic population model (equations (1)–(3)) was suitable for investigating large population dynamics under drug treatment, the corresponding stochastic population model (equations (7)–(15)) was necessary to accurately quantify fixation time and mutation first-appearance time distributions and extinction events for cidal drug treatment scenarios, where the total population size becomes small enough to result in extinction events (no drug resistance mutation appears before S and N reach zero). When starting with no pre-existing mutations ($G_i = 0$), the fixation times calculated using the deterministic model of cidal drug treatment tended to be underestimated compared to those calculated using averages over exact stochastic simulations. When starting with a pre-existing mutation ($G_i = 1$), the average fixation times using the stochastic model converged to the those found using the deterministic model (appendix H). This

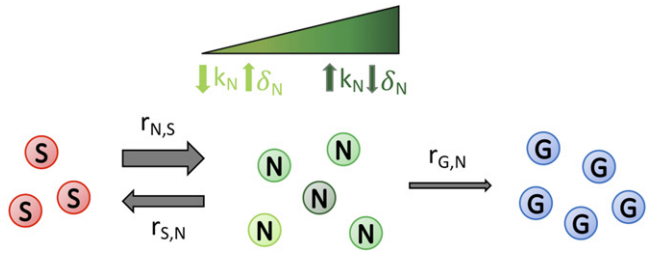

Figure 1. Schematic depicting the transitions between susceptible, non-genetically resistant, and genetically resistant subpopulations in a cell population undergoing drug treatment. Cells with the drug susceptible (S) phenotype can switch to non-genetically drug-resistant (N) phenotype and vice versa (at rates $r_{N,S}$ and $r_{S,N}$, respectively). The degree of susceptibility or resistance of S, N, and G to a drug can be varied between simulations and is dependent on the treatment scenario being investigated. For example, a higher birth rate (k_N) or a lower death rate (δ_N) results in the degree of transient drug resistance of N cells being higher (represented by dark green cells), whereas a lower k_N or a higher δ_N results in a lower level of transient drug resistance (represented by light green cells), as described overall by the fitness (N subpopulation growth rate) in the presence of a static or cidal drug, respectively; this is similar, but not shown in the schematic for clarity, for S and G cells. Cells from the N subpopulation can mutate (at a rate $r_{G,N}$) to become permanently genetically drug-resistant (G) cells.

highlights the importance of stochastic modeling when considering low numbers of infectious cells with no pre-existing drug resistance mutations.

We focus on the cidal drug treatment scenario for stochastic simulations for constant and fluctuating drug conditions, as the corresponding static drug stochastic simulations took prohibitively long to simulate due the lack of cell death, which resulted in larger subpopulation/population sizes, and correspondingly stochastic fluctuations were not expected to have much effect on the population dynamics.

3. Results and discussion

The parameters for the deterministic and stochastic population models are provided in appendix A (table A1) and the simulation codes are freely available at: https://github.com/CharleboisLab/S-N-G.

3.1. Deterministic population and evolutionary dynamics under static drug exposure

We began by numerically solving the deterministic population model to generate the time series subpopulation concentrations to investigate the relative fitness effects of the non-genetically and genetically resistant subpopulations on the evolution of drug resistance during static drug treatment. We model the effects of a static drug by setting the birth rate of the susceptible cells S to zero ($k_S = 0$) and setting all death rates to a natural basal death rate, which was based on the chronological life span of *S. cerevisiae* (table A1) [45].

The concentration of S initially decreases after the application of the static drug as a result of cells switching from S to N and then increases logistically due to switching from N to S, before falling toward extinction due to resource competition with the G subpopulation (figure 2(A)). The growth of N follows a logistic-type curve before also falling toward extinction (figure 2(B)). Overall, the growth of S and N (figures 2(A) and (B)), along with the growth of total population (figure 2(D)), increase as the fitness of N increases (modeled for static drug treatment by increasing the birth rate of N).

The concentration of G (figure 2(C)) and the fraction of G in the total population (figure 2(E)) reveal that an increase in the fitness of N slows the expansion of G. This can be attributed to resource competition between the subpopulations, as a higher total population size reduces the growth rate of G (equation (6)).

The growth rate of the total population over time increases before sharply decreasing after it reaches a maximum (figure 2(F)). This is a result of the growth of the population beginning to slow down as it increases in size ($\mathrm{d}T/\mathrm{d}t \to 0$ as $T \to \infty$), which is expected for logistic-type growth [37]. Despite the decrease in the expansion of G, the total population growth rate increases as the fitness of N increases (figure 2(F)). Thus, increasing the fitness of N in the static drug environment enhances the growth of the population, while at the same time hindering the expansion of G. Additionally, intense resource competition drives the S and N subpopulations to extinction at longer timescales.

Then, we quantified how the fitness of the N and G subpopulations affect the fixation of the mutated G subpopulation. As expected, an increase in k_G relative to k_N shortens the fixation time of G in the population (figure 3(A)). Importantly, increasing k_N relative to k_G lengthens the fixation time of G (figure 3(A)), due to competition decreasing the fraction of G in the total population (figure 2(E)).

Overall, the trends in the static drug environment were similar for a wide range of mutation rates (figure F5), though there were some qualitative differences for variations in the S–N switching rates (figures F1 and F2) (appendix F).

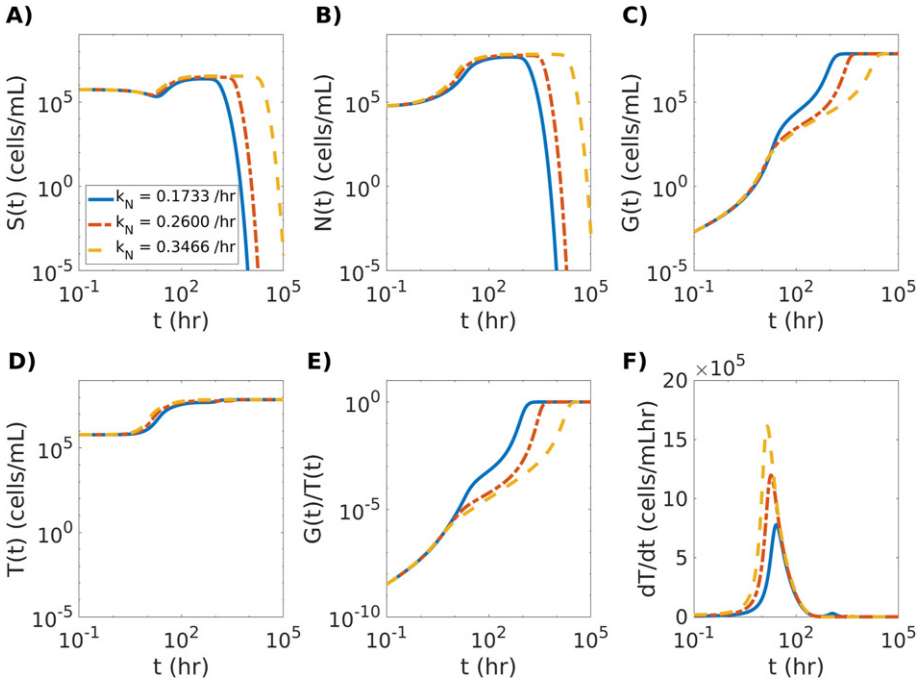

Figure 2. Growth of the genetically resistant subpopulation is hindered by an increase in birth rate of the non-genetically resistant subpopulation during static drug treatment. (A) The growth curve of the susceptible (S) subpopulation. (B) The growth curve of the non-genetically resistant (N) subpopulation. (C) The growth curve of the genetically resistant (G) subpopulation. (D) The growth curve of the total population (T). (E) The fraction of G in the total population (T). (F) The rate of change in the size of T (dT/dt) as a function of time (t). Each coloured line represents a different numerical simulation corresponding to the growth value of N (k_N) shown in the legend in (A), with the solid blue line representing the lowest level of N fitness ($k_N = 0.1733\ h^{-1}$), the red dash-dotted line an intermediate level of N fitness ($k_N = 0.2600\ h^{-1}$), and the yellow dashed line the highest level of N fitness ($k_N = 0.3466\ h^{-1}$) relative to the fitness of G ($k_G = 0.3466\ h^{-1}$) when exposed to a static drug.

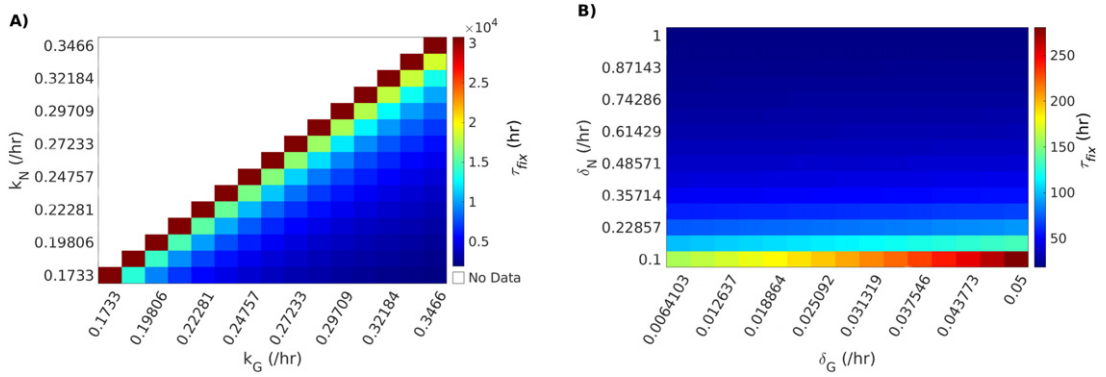

Figure 3. Drug resistance of the non-genetic subpopulation slows the evolution of the genetically resistant subpopulation during drug exposure. (A) Heat map shows the effect of the birth rates of the non-genetically resistant (N) and genetically resistant (G) subpopulations (k_N and k_G, respectively) on the fixation time (τ_{fix}) of the genetically resistant subpopulation (G) during static drug treatment. (B) Heat map shows the effect of the death rates of N and G (δ_N and δ_G, respectively) on the τ_{fix} of G during cidal drug treatment. For this case, we set δ_S was set to 1.0 h^{-1} and k_N and k_G to 0.3466 h^{-1}. Each bin in (A) and (B) corresponds to a simulation for a particular combination of k_N and k_G or δ_N and δ_G, respectively. The colour bar gives τ_{fix} in hours. As k_N is less than or equal to k_G, numerical simulation data does not appear in the upper diagonal of the heat map in (A).

3.2. Deterministic population and evolutionary dynamics under cidal drug exposure

Next, we investigated how the relative fitness of the non-genetically resistant and genetically resistant subpopulations affected the evolutionary dynamics of the population under cidal drug treatment.

The concentration of S quickly declines after exposure to the cidal drug, with phenotype switching from N providing temporary survival before dying off (figure 4(A)). The N subpopulation shows temporary growth for lower values of δ_N before dying off, while higher values of δ_N produce flat growth curves before going extinct due to drug treatment and subpopulation competition (figure 4(B)). Lower δ_N values (higher N fitness) prolong the temporary survival of S and N compared to higher δ_N values (figures 4(A) and (B)). The logistic growth of G also changes due to the fitness of N, with the higher δ_N (lower N fitness)

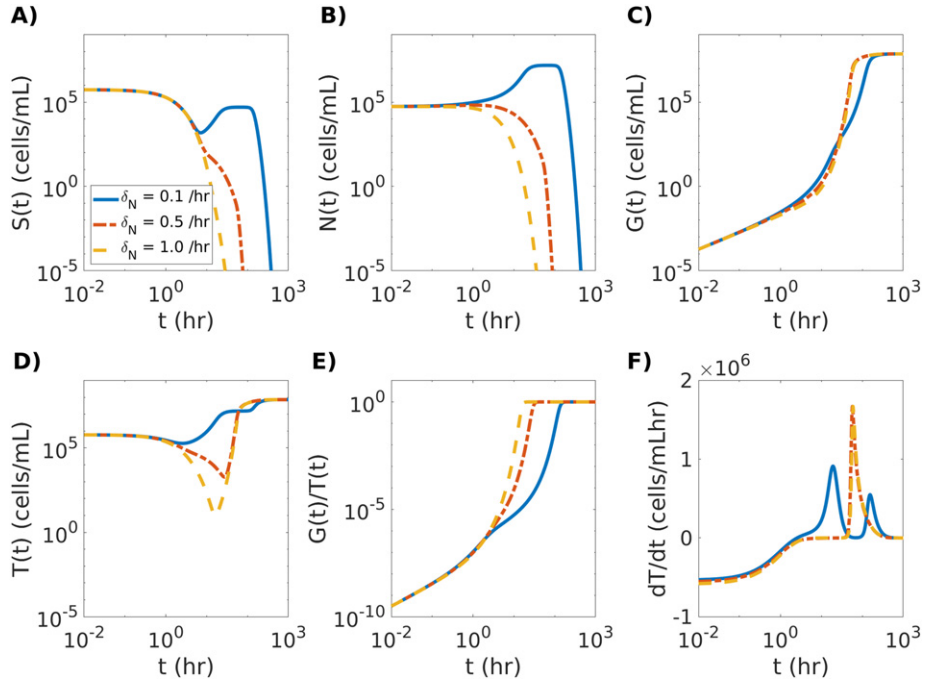

Figure 4. The fraction of the genetically resistant cells in the population increases with a decrease in fitness of the non-genetically resistant subpopulation in a cidal drug environment due to intraspecific competition. (A) The growth curve of the drug susceptible (S) subpopulation. (B) The growth curve of the non-genetically drug resistant (N) subpopulation. (C) The growth curve of the genetically drug resistant (G) subpopulation. (D) The growth curve of the total population (T). (E) The fraction of G in the total population (T). (F) The rate of change in the size of T (dT/dt) as a function of time (t). Each coloured line represents a different numerical simulation corresponding to the death rates of N shown in the legend in (A), with the solid blue line representing the highest level of N fitness (death rate of 0.1 h^{-1}), the red dash-dotted line an intermediate level of N fitness (death rate of 0.5 h^{-1}), and the yellow dashed line the lowest level N fitness (death rate of 1.0 h^{-1}) relative to the fitness of G (unaffected by the drug) during cidal drug treatment. S was given a death rate of 1.0 h^{-1} for these simulations, and the birth rate of both N and G was set to 0.3466 h^{-1}.

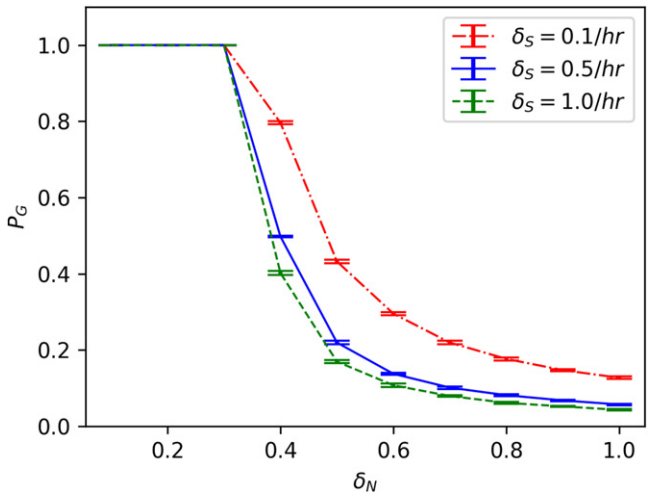

Figure 5. Probability of genetic drug resistance emerging before population extinction increases with the fitness of the non-genetically resistant subpopulation during cidal drug treatment. The appearance probability of the genetically drug resistant subpopulation (P_G) is shown as a function of decreasing N fitness (death rate; δ_N). Each coloured line represents a different strength of the cidal drug on the susceptible population S, with the red dashed-dotted line representing the lowest strength ($\delta_S = 0.1$ h^{-1}), the blue line an intermediate strength ($\delta_S = 0.5$), and the green dashed-dotted line the highest strength ($\delta_S = 1.0$ h^{-1}). The birth rates of N and G were set to $k_N = k_G = 0.3466$ h^{-1}. Each data point is an average over ten realizations of 10 000 simulations. Error bars show the standard deviation.

values producing a sharper increase toward saturation (figure 4(C)). Increasing the fitness of N decreases the fraction of G in the total population, as lower δ_N values result in more N cells and consequently lower G/T values (figure 4(E)).

The number of cells in the total population initially declines (negative growth rate; figure 4(D)) before stabilizing at zero population growth (figure 4(F)). Then the population growth rate increases as the genetically drug resistant G subpopulation

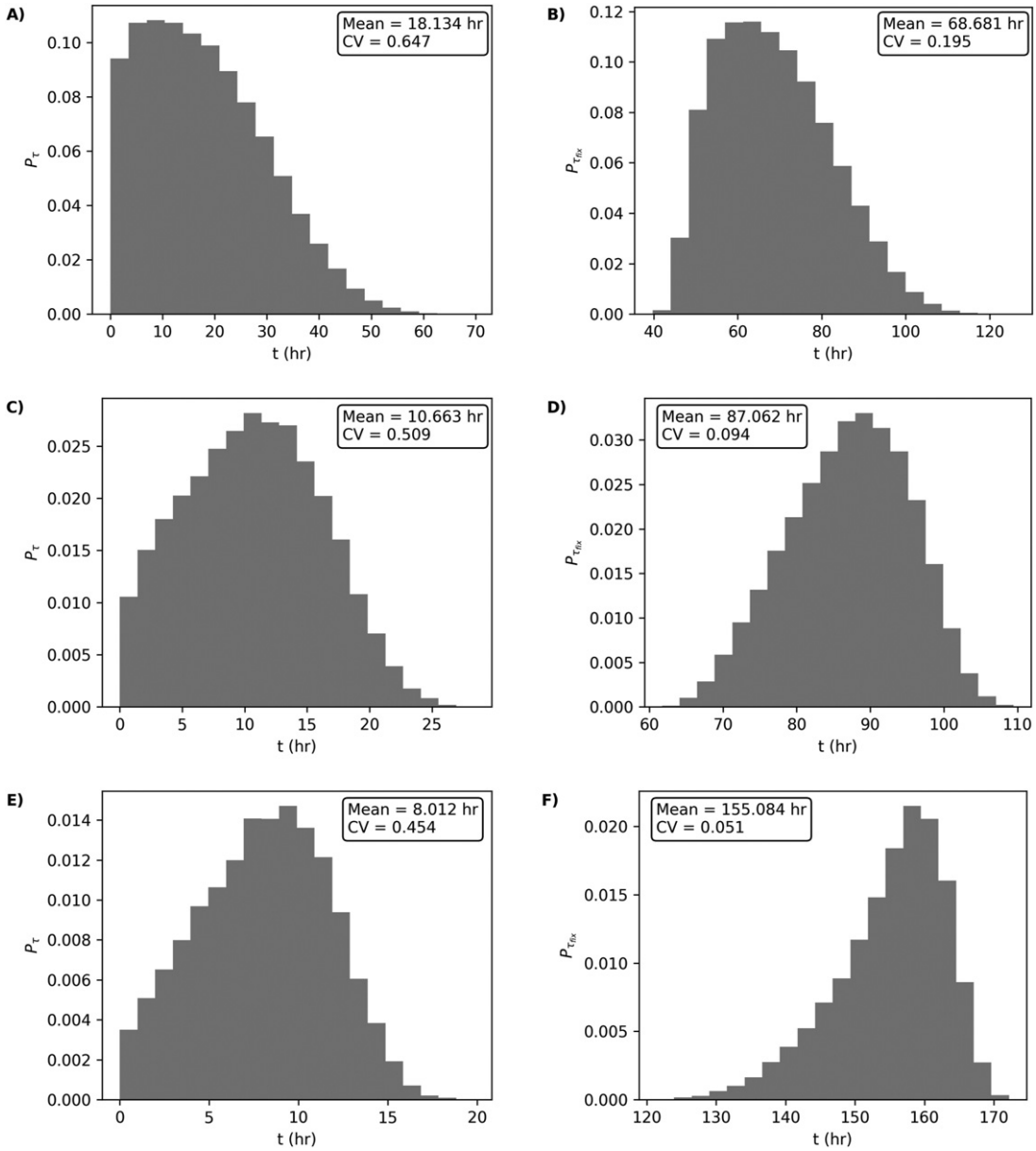

Figure 6. Drug resistance mutation first-appearance time and fixation time distributions during cidal drug treatment. (A) First-appearance time (P_τ) and (B) fixation time ($P_{\tau_{\text{fix}}}$) distributions for the genetically resistant subpopulation (G) for a low level of non-genetically resistant subpopulation (N) fitness (death rate; $\delta_N = 0.3\ \text{h}^{-1}$). For (A) and (B), histograms show results for 14 625 stochastic simulations. (C) P_τ and (D) $P_{\tau_{\text{fix}}}$ distributions for G for an intermediate level of N fitness ($\delta_N = 0.2\ \text{h}^{-1}$). For (C) and (D), histograms show results for 30 391 SSA simulations. (E) P_τ and (F) $P_{\tau_{\text{fix}}}$ distributions for G for a high level of N fitness ($\delta_N = 0.1\ \text{h}^{-1}$). For (E) and (F), histograms show results for 100 000 stochastic simulations. The mean and the CV for each distribution is provided in the top corners of each plot. The death rate of S was set to $\delta_S = 1.0\ \text{h}^{-1}$ and the birth rates of N and G were set to $k_N = k_G = 0.3466\ \text{h}^{-1}$ for these simulations.

expands to take over the population. This is followed by a decrease in the population growth rate, as the total population size moves toward saturation (zero population growth) after the maximum population growth rate is reached. Interestingly, when the fitness of N was high, there was a subsequent resurgence in the population growth rate before the population finally saturates. The first peak in the population growth rate is a due increasing S and N concentrations, and the second peak is due to a subsequent rising in G subpopulation concentration. When G is considered to be partially resistant (i.e. $\delta_G > 1/156\ \text{h}^{-1}$), cidal drug treatment can either drive the total population to extinction or result in non-zero steady-state S, N, and G subpopulation concentrations (figure E1).

As for the static drug treatment, increasing the fitness of N hinders the fixation time of the genetically resistant subpopulation during cidal drug treatment (figure 3(B)). Similar population dynamics were observed when N was given a smaller birth rate ($k_N = 0.1733\ \text{h}^{-1}$) compared to G (figure D1). Overall, the findings for cidal drug treatment were qualitatively similar for a wide range of parameters (figures C1, F3, F4, and F6) (appendix F).

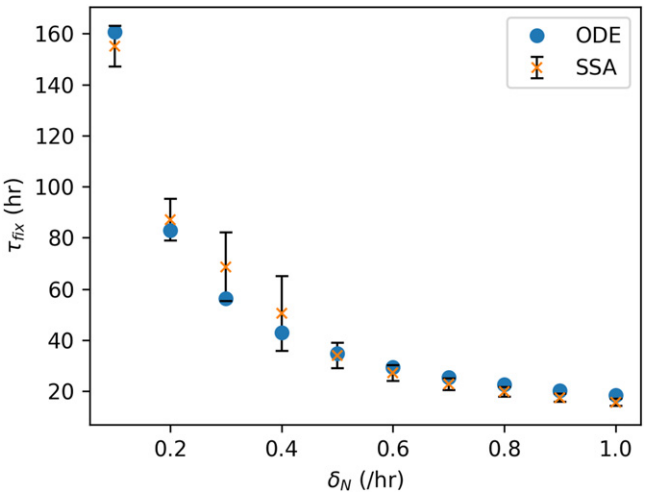

Figure 7. Fixation time of a genetic resistance mutation as a function of non-genetic drug resistance. Shown are the numerical solutions of the deterministic ODE model (blue dots) and SSA results (orange crosses) for the corresponding stochastic model. The death rate of the susceptible population (S) was set to $\delta_S = 1.0\ \mathrm{h}^{-1}$ and the birth rates of N and G were set to $k_N = k_G = 0.3466\ \mathrm{h}^{-1}$ for these simulations. Error bars on the SSA results denote the standard deviation.

3.3. Stochastic evolutionary dynamics during cidal drug treatment

We simulated the stochastic population model (equations (7)–(15)) translated from the deterministic population model (equations (1)–(3)) to investigate the transition from non-genetic to genetic drug resistance in cell populations moving toward extinction during cidal drug treatment. This is important as fluctuations in small subpopulation sizes may impact the evolutionary dynamics of the population. Given that S and N are killed to differing degrees by the cidal drug, and that the evolution of G depends directly on N, we hypothesized that stochastic fluctuations in the size of N could lead to the survival or extinction of the total population. To quantify the population and evolutionary drug resistance dynamics in this regime, we determined how the fitness of N affects the probability of population extinction (which occurs when S and N go extinct before G emerges; figure G1), along with the first-appearance and fixation times of a genetic mutation, which are bound to occur in our model once G is present in the population.

Decreasing the fitness of N (increasing δ_N) decreased the likelihood of G appearing and rescuing the cell population from extinction during cidal drug treatment (figure 5). This is in qualitative agreement with a previous study that found that increasing the fluctuation relaxation time of a drug resistance gene increased the probability of acquiring a drug resistance mutation [6]. When N had high fitness in the cidal drug environment ($\delta_N = 0.1\ \mathrm{h}^{-1}$ to $\delta_N = 0.3\ \mathrm{h}^{-1}$) the total population never went extinct. The extinction probability increased exponentially as the fitness of N decreased, with the population going extinct between 57% and 83% (depending on the value of δ_S) of the time for moderate fitness ($\delta_N = 0.5\ \mathrm{h}^{-1}$), and between 87% and 96% (depending on the value of δ_S) of the time for low fitness ($\delta_N = 1.0\ \mathrm{h}^{-1}$). These results show that the presence of non-genetic resistance enhances population survival when there are no pre-existing drug resistance mutations prior to drug exposure, and that non-genetic resistance increases the chance that a mutation will occur by providing a drug-exposed population with more time before extinction. As expected, G always appeared in the population when the strength of the cidal drug was low ($\delta_N < 0.3\ \mathrm{h}^{-1}$), and conversely, the population almost always went extinct before G could emerge when the strength of the cidal drug was high ($\delta_N = 1.0\ \mathrm{h}^{-1}$) (figure 5).

When the fitness of N increased in the cidal drug environment so did the means of the mutation first-appearance time and fixation time distributions (figure 6). This indicates that the presence of non-genetic drug resistance slows the evolution of genetic drug resistance, in agreement with the results obtained from the deterministic population model (figure 3(B)). While the coefficient of variation (CV; defined as the standard deviation divided by the mean) of the first-appearance time distributions (figures 6(A), (C) and (E)) was only marginally dependent on the fitness of N, the CV of the fixation time distributions (figures 6(B), (D) and (F)) increased approximately three fold as the fitness of N increased from low to high. Therefore, the presence of increased non-genetic drug resistance is predicted to not only slow down genetic drug resistance, but also to increase the uncertainty in its evolution.

A comparison of the fixation times found using the deterministic ODE model and the mean fixation times calculated over many stochastic simulation algorithm (SSA) simulations for various δ_N values

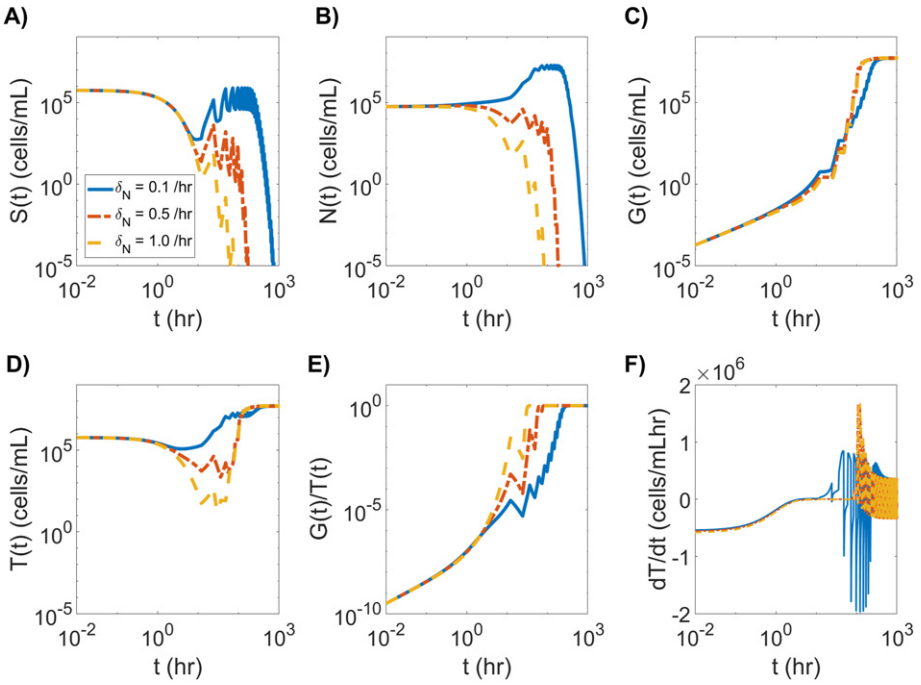

Figure 8. Oscillatory subpopulation concentration and growth rate dynamics in alternating drug-no drug conditions. The fraction of the genetically resistant cells in the population increases with the death rate of the non-genetically resistant subpopulation in a fluctuating cidal drug environment (12 h alternating drug-no drug intervals, starting with the drug applied). (A) The growth curve of the drug susceptible (S) subpopulation. (B) The growth curve of the non-genetically drug resistant (N) subpopulation. (C) The growth curve of the genetically drug resistant (G) subpopulation. (D) The growth curve of the total population (T). (E) The fraction of G in the total population (T). (F) The rate of change in the size of T ($\mathrm{d}T/\mathrm{d}t$) as a function of time (t). Each coloured line represents a different numerical simulation corresponding to the death rates of N shown in the legend in (A), with the solid blue line representing the highest level of N fitness (death rate of 0.1 h^{-1}), the red dash-dotted line an intermediate level of N fitness (death rate of 0.5 h^{-1}), and the yellow dashed line the lowest level N fitness (death rate of 1.0 h^{-1}) relative to the fitness of G (unaffected by the drug) during cidal drug treatment. S was given a death rate of 1.0 h^{-1} for these simulations, and the birth rate of both N and G was set to 0.3466 h^{-1}.

is shown in figure 7. As expected, the mean fixation times calculated from the stochastic simulations generally match those found using the deterministic model. When modeling a pre-existing mutation ($G_i = 1$), which removes the stochasticity in the first appearance time of the mutant subpopulation, the mean values of the stochastic simulation results converge with those found using the deterministic model (figure H1). Importantly, both deterministic and stochastic models show that decreasing the fitness of N increases the speed of genetic fixation (this also holds for pre-existing mutation scenarios; figure H1).

3.4. Evolutionary dynamics during fluctuating cidal drug treatment

To investigate evolutionary drug resistance dynamics in fluctuating drug treatment scenarios, we assigned resistant subpopulations a fitness cost when the drug was removed. This was done by reducing k_N to 0.2600 h^{-1} and k_G to 0.1733 h^{-1}, while allowing S to grow with $k_S = 0.3466$ h^{-1} in the no-drug environment (which also opened the mutational pathway from S to G at a rate $r_{G,S}$); the parameters were the same as before in the intervals where the cidal drug was applied (table A1).

We first performed deterministic simulations where drug application intervals ranged from 6 to 48 h, followed by no-drug intervals of the same duration. The fraction of G in the total population changes relative to the fitness of N in a similar way as the constant drug environment, showing a hindrance of the fixation of G with increasing N fitness (figures 8 and 9). Alternating between drug and no-drug environment resulted in oscillations in the subpopulation concentrations and population growth rate (figure 8). Interestingly, when N had a high level of resistance to cidal drug treatment, the population growth rate oscillated dramatically before saturating, rather than the isolated population growth rate surge and resurgence peaks that occurred prior to saturation in the constant cidal drug environment simulations (figure 8(F)). Increasing the period of the drug–no drug fluctuations also lengthens the fixation time scales of G (figure 9) compared to the constant cidal drug treatment scenario (figure 3(B)). Thus, fluctuating the drug condition, along with the presence of non-genetic drug resistance, can length the onset of permanent genetic drug resistance.

Next, we performed stochastic simulations to determine the probability of genetic drug resistance appearing before population extinction for 12, 24, and 48 h fluctuations in cidal drug treatment.

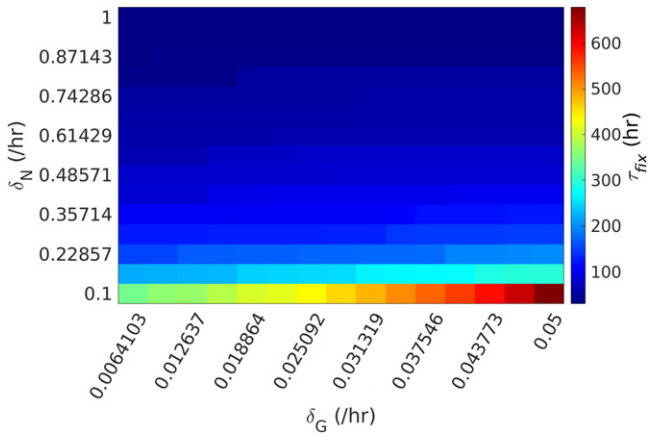

Figure 9. Drug resistance of the non-genetic subpopulation slows the evolution of the genetically drug resistant subpopulation during fluctuating cidal drug exposure. Heat map shows the effect of the death rates δ_N and δ_G on the τ_{fix} of G during cidal drug treatment for 12 h drug–no drug fluctuations time, starting with drug applied. δ_S was set to 1.0 h^{-1}, as it was assumed that S would experience the least amount of resistance to the drug compared to N and G, and the trends seen here were found to hold for fluctuation times of 6–48 h (data not shown). Each bin corresponds to a simulation for a particular combination of δ_N and δ_G. The colour bar gives τ_{fix} in hours.

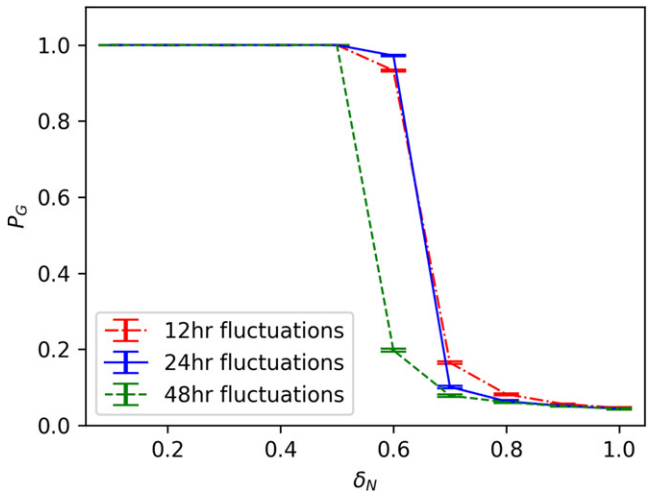

Figure 10. Probability of genetic drug resistance emerging before population extinction decreases at longer cidal drug–no cidal drug fluctuation intervals. The appearance probability of the genetically drug resistant subpopulation (P_G) is shown as a function of N fitness (death rate; δ_N). Each coloured line represents a different fluctuation time, with the red dashed-dotted line representing 12 h fluctuations, the blue line 24 h fluctuations, and the green dashed-dotted line 48 h fluctuations (each starting with drug applied). Each data point is an average over ten realizations of 10 000 simulations. Error bars show the standard deviation.

Importantly, increasing the fluctuation timescale of the drug to 48 h decreases the probability of genetic drug resistance emerging at intermediate levels of δ_N, compared to 12 and 24 h drug–no drug fluctuation intervals (figure 10). As in the constant cidal drug scenario, decreasing the fitness of the non-genetically resistant subpopulation lowers the chance of G appearing before population extinction.

Overall, these results suggests that alternating drug conditions can result in oscillatory population dynamics, and that increasing the drug–no drug timescales can increase resistance mutation fixation times and decrease population survival.

4. Conclusion

We found using deterministic and stochastic population models that while non-genetic resistance enhances population survival, a slower rate of genetic resistance evolution emerges from resource competition between these subpopulations during constant and fluctuating drug treatments. Specifically, increasing the fitness of the non-genetically resistant subpopulation (which allows the population to survive initial drug exposure) exponentially increased the chance of a genetically resistant subpopulation appearing and rescuing the total population from

extinction during treatment at intermediate cidal drug strength. However, increasing the fitness of the non-genetically resistant subpopulation, along with fluctuating the drug condition, slowed down the fixation time of the genetic drug resistance mutation due to subpopulation competition effects, when no pre-existing mutations were present in the population. Incorporating pre-existing mutations into the model reduced the timescale of fixation, as it removed the growth delay resulting from the time taken by non-genetically resistant cells to mutate into genetically resistant cells. For the stochastic simulations, the presence of pre-existing mutations reduced the stochasticity of the first-appearance time of the genetically resistant subpopulation and protected against population extinction. Corresponding experimental investigations could be performed using microbes harbouring inducible synthetic gene circuits to control the fraction of non-genetically resistant cells in the population in combination with DNA sequencing to track the appearance time and frequency of drug resistance mutations [31–33].

High levels of competition drove the competing susceptible and non-genetically resistant subpopulations extinct in static and cidal drug treatment scenarios, which opens the possibility of incorporating competition and resource limitation strategies into antimicrobial therapies. These predictions could be tested experimentally, for instance through competition assays [46] in which synthetic gene circuits tune the initial fractions of susceptible and non-genetically drug resistant cells in the population [31].

Alternating drug–no drug conditions generated oscillatory population dynamics, and increasing the drug–no drug fluctuation timescale resulted in lengthened resistance mutation fixation times and a sharper population survival-extinction 'phase transition'. It will be important to investigate the effects of non-genetic resistance on the development of genetic resistance in more complex cell models [47] and further in the context of fluctuating environments, which may be governed by environment-sensing genetic networks [48], along with cellular trade-offs that may occur in drug environments [49]. Microfluidic devices could be used to experimentally study the effects of fluctuating drug stress at the single-cell level [50, 51]. Fluctuating environmental stressors have been shown to facilitate 'bet-hedging' in cell populations [52, 53], whereby some cells adopt a non-growing, stress-resistant phenotype to increase the long-term fitness of the population. This could be modelled using stochastic hybrid processes [54], for instance by using an stochastic ON–OFF switch coupled to a system of ODEs describing subpopulation dynamics in the presence of a drug. Furthermore, the first-appearance time, fixation time, and extinction events could be described analytically in future studies using a first-passage time framework [6, 55].

Overall, our quantitative model generated robust and novel predictions on the evolution of drug resistance, and revealed that the interplay between transient non-genetic drug resistance and permanent genetic resistance may be more complex than previously thought. Specifically, in addition to enhancing the survival of a drug-exposed microbial population in constant drug conditions [4, 5, 10, 16, 24], our findings demonstrate that transient non-genetic resistance may hinder the evolution of permanent genetic resistance in constant and fluctuating drug conditions. As drug exposure is generally a form of selective pressure, the results of this study are also anticipated to be useful for understanding the evolutionary dynamics of other stress-resistant microbial populations.

A complete understanding of the drug resistance process, including the interplay between non-genetic and genetic forms of drug resistance, will be important for mitigating the socio-economic costs of antimicrobial resistance [5]. The resistance mutation appearance probabilities and first-appearance time distributions determined using stochastic population models may prove useful for guiding drug therapies. Quantitative distributions such as these may someday serve as a way to avoid drug failure resulting from the transition from non-genetic to genetic resistance by indicating the timescale at which a clinician should substitute or combine drugs during treatment to avoid the selection of resistance-conferring mutations [56, 57]. Fluctuations in mutation first-appearance times are also important, as they can be the difference between the eradication or the establishment of drug-resistant infection during drug therapy. Finally, drug resistant infections may one day be overcome by novel strategies that enhance competition between non-genetically and genetically resistant pathogens during treatment. One potential strategy is to revert an infectious population of cells from being drug-resistant to drug-sensitive by periodically fluctuating the drug environment. Specifically, by temporarily removing or substituting the drug, the fitness costs associated with subpopulation competition considered in our study, along with the previously established costs of non-genetic resistance [9, 32] and resistance mutations [58], could be exploited such that drug-susceptible cells dominate in the population. Overall, improving our quantitative understanding of how non-genetic and genetic mechanisms interact will advance our fundamental understanding of drug resistance evolution and may lead to more effective treatments for patients with drug-resistant infections.

Acknowledgements

DC was financially supported by the Government of Canada's New Frontiers in Research Fund—Exploration program (2019-01208), a Natural Sciences and Engineering Research Council of Canada (NSERC) Discovery Grant (RGPIN-2020-04007), an NSERC Discovery Launch Supplement (DGECR-2020-00197), and the University of Alberta. JG was supported by a 2021 NSERC Undergraduate Student Research Award.

Author contributions

DC conceived, designed, and supervised the research. DC developed the mathematical models. JG carried out the numerical and stochastic simulations. JG and DC analysed the data. DC and JG wrote the article.

Conflict of interest

The authors have no conflicts of interest to declare.

Data availability statement

The data that support the findings of this study are openly available at the following URL/DOI: https://github.com/CharleboisLab/S-N-G.

Appendix A. Parameters

The parameter values used in our study (table A1) were based on experimental studies on the budding yeast *S. cerevisiae* [32, 33, 45, 59, 60]. Additionally, some parameters were scanned over a range of values to account for parameter uncertainty, to probe for parameter regime specific model behaviour, and to test the robustness of the simulation results.

Drug susceptible cells S formed the majority of the total initial population (T_i) and non-genetically drug resistant cells N formed 1%–10% of T_i [19]. We assumed there were no pre-existing genetic drug resistance mutations ($G_i = 0$) for all numerical and stochastic simulations in the main text. Numerical simulation of the deterministic population started with $S_i = 5.5 \times 10^5$ cells ml^{-1} and $N_i = 5.5 \times 10^4$ cells ml^{-1}, which are common initial concentrations for 'log-phase' laboratory experiments [60].

Depending on the concentration of the drug being considered, constant birth rates k_N and k_G (which model the fitness of the given subpopulation in the presence of a static drug where death rates are unaffected) were assigned values between 0.1733 h^{-1} and 0.3466 h^{-1}, based on birth rates measured in standard yeast cell culture experiments [59]. For cidal drugs, we modeled fitness by setting the birth rates k_N and k_G equal and scanning over N and G death rates (δ_N and δ_G) at a constant S death rate (δ_S); the trends also held for lower k_N and δ_S values (see appendix C and appendix D). The parameter ranges in table A1 were the basis of parameter scans that were used to predict how the relative fitness between N and G will affect population dynamics and the evolution of genetic drug resistance in our study.

To model partial drug resistance due to gene-expression noise, it was assumed that $k_N \leqslant k_G$ for static drugs and $\delta_G \leqslant \delta_N$ for cidal drugs, with genetic drug resistance mutations providing the greatest level of resistance. Genetic mutations were also assumed to be permanent in our simulations.

The switching rates between S and N are based on experimental estimates [32] and ranged between $r_{S,N} = 0.0035$ h^{-1} and $r_{N,S} = 0.0625$ h^{-1}. The mutation rate from N to G was based on a previous modeling-experimental study [19], which ranged from 10^{-6} to 10^{-7} per cell division, and was assigned a value of $r_{G,N} = 0.3 \times 10^{-6}$ h^{-1} in our simulations.

The deterministic and stochastic population models provide a means to simulate the effects of non-genetic resistance on the evolution of drug resistance. The effects of static drugs (which reduce cell growth but do not kill cells) were modeled by arresting the birth of S ($k_S = 0$ and $r_{G,S} = 0$) and varying the birth rates of N and G (k_N and k_G, respectively) and by setting the death rates to a low natural basal death rate ($\delta_S = \delta_N = \delta_G = 1/156$ h^{-1}). Cidal drugs (which eventually kill all non-genetically resistant cells) were modeled by adding non-zero death rates for S and N (δ_S and δ_N, respectively). Unless otherwise stated, we also modeled partial drug resistance of N by setting $\delta_N < \delta_S$. Overall, varying key parameters specified in table A1 did not yield qualitatively different results.

The parameter values given in table A1 were also used for the stochastic simulations, as all the corresponding reactions in the stochastic population model were of zeroth-order or first-order [37]. Note that in the stochastic population model the values of S_i, N_i, and G_i are exact numbers of cells ($S_i = 5.5 \times 10^5$ cells and $N_i = 5.5 \times 10^4$ cells), which we used as the initial conditions to investigate the stochastic transition from non-genetic to genetic resistance as the number of cells in the population approached zero (extinction) due to cidal drug treatment. The S to N (and vice-versa) phenotype switching rates ($r_{N,S}$ and $r_{S,N}$, respectively), the N to G mutation rate ($r_{G,N}$), and the birth and death rates (k_i and δ_i, respectively, where $i \in \{S, N, G\}$) are all given as probability per unit time in the stochastic population model.

Table A1. Parameters used for numerically simulating the deterministic population dynamics model in static and cidal drug conditions. A horizontal line in the 'cidal drug value' column indicates that the value is the same as the corresponding value in the 'static drug value' column. A blank entry in the 'units' column indicates no units and 'see text' in the 'reference' indicates that the justification for the parameter value is given in the main text or appendices.

Parameter	Static drug value	Cidal drug value	Units	Reference
S_i	5.5×10^3 to 5.5×10^8	—	Cells ml^{-1}	[60]
N_i	5.5×10^2 to 1.1×10^8	—	Cells ml^{-1}	[9, 19]
G_i	0	—	Cells ml^{-1}	[39]
k_S	0	—	h^{-1}	[39]
k_N	0.1733–0.3466	—	h^{-1}	[59]
k_G	0.1733–0.3466	—	h^{-1}	[59]
$r_{S,N}$	0.0035	—	h^{-1}	[32, 33]
$r_{N,S}$	0.0625	—	h^{-1}	[32, 33]
$r_{G,S}$	0	—	h^{-1}	[39]
$r_{G,N}$	$10^{-6}/3$	—	h^{-1}	[19]
δ_S	1/156	0.1–1.0	h^{-1}	[45]
δ_N	1/156	0.1–1.0	h^{-1}	[45]
δ_G	1/156	1/156–0.05	h^{-1}	[45]
h	1×10^7	—	Cells ml^{-1}	See text
n	2	—		[59]

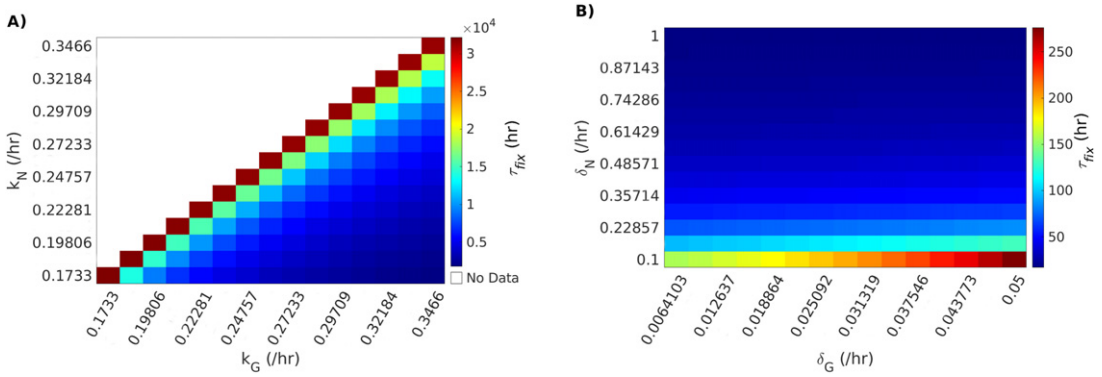

Figure B1. Simulations with a small S birth rate of $k_S = 0.01$ h^{-1} and a mutational pathway from S to G (with a mutation rate $r_{G,S}$ equal to $r_{G,N}$ used previously). (A) Fixation time heatmap for static drug case. (B) Fixation time heatmap for cidal drug case (with $\delta_S = 1.0$ h^{-1}).

Appendix B. Small S birth rate and mutational pathway from S to G

To test the scenario where drugs hinder but do not completely arrest growth of the susceptible cells S, we ran simulations with a small birth rate k_S. We also considered an active mutational pathway from S to G (with the mutation rate $r_{G,S}$ being equal to the $r_{G,N}$ mutation rate used in the main text). For all values of k_S tested (ranging from 1% to 50% the growth rates used in the main text), the main conclusion that non-genetic resistance hinders the fixation of resistance mutations held for static and cidal drug scenarios. A representative case for $k_S = 0.01$ h^{-1} is provided for the static drug case in figure B1(A) and for the cidal case in figure B1(B). Specifically, there were small quantitative differences in fixation times, but the qualitative relationship between fixation time and k_N or δ_N held.

Appendix C. Different cidal drug strengths

Figure C1 demonstrates that the qualitative results discussed in the main text hold for higher levels of S fitness (death rate $\delta_S = 0.5$ h^{-1} and $\delta_S = 0.1$ h^{-1}) in the cidal drug environment. Figure C1(A) shows the cidal drug fixation heatmap using the deterministic ODE model for an intermediate S fitness of $\delta_S = 0.5$ h^{-1} and figure C1(B) shows the same case for a high S fitness of $\delta_S = 0.1$ h^{-1}. The finding that the fitness of the S subpopulation had little effect on the fixation of G in the cidal drug environment can likely be attributed to the fact that $k_S = 0$ makes the

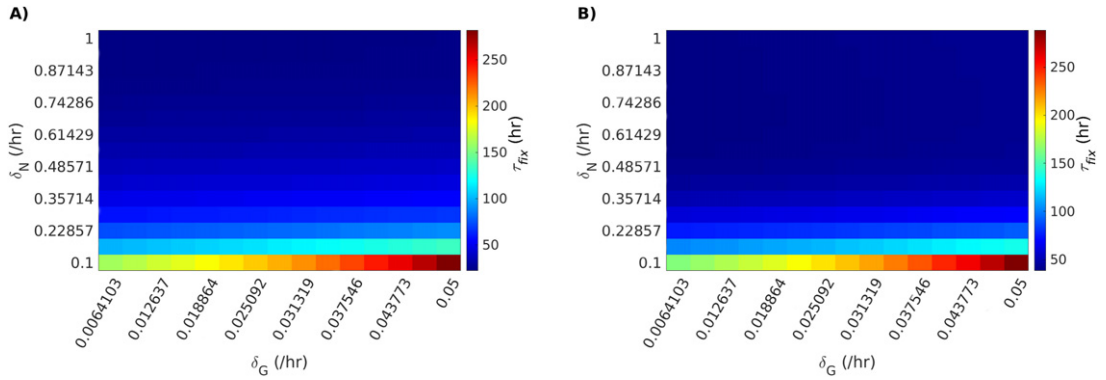

Figure C1. The results in the main text regarding N fitness and G fixation are shown to hold for higher levels of S fitness than those considered in the cidal drug environment in the main text ($\delta_S = 1.0\ \mathrm{h}^{-1}$; figure 3(B)). (A) Fixation time heatmap for intermediate S fitness ($\delta_S = 0.5\ \mathrm{h}^{-1}$). (B) Fixation time heatmap for higher S fitness ($\delta_S = 0.1\ \mathrm{h}^{-1}$).

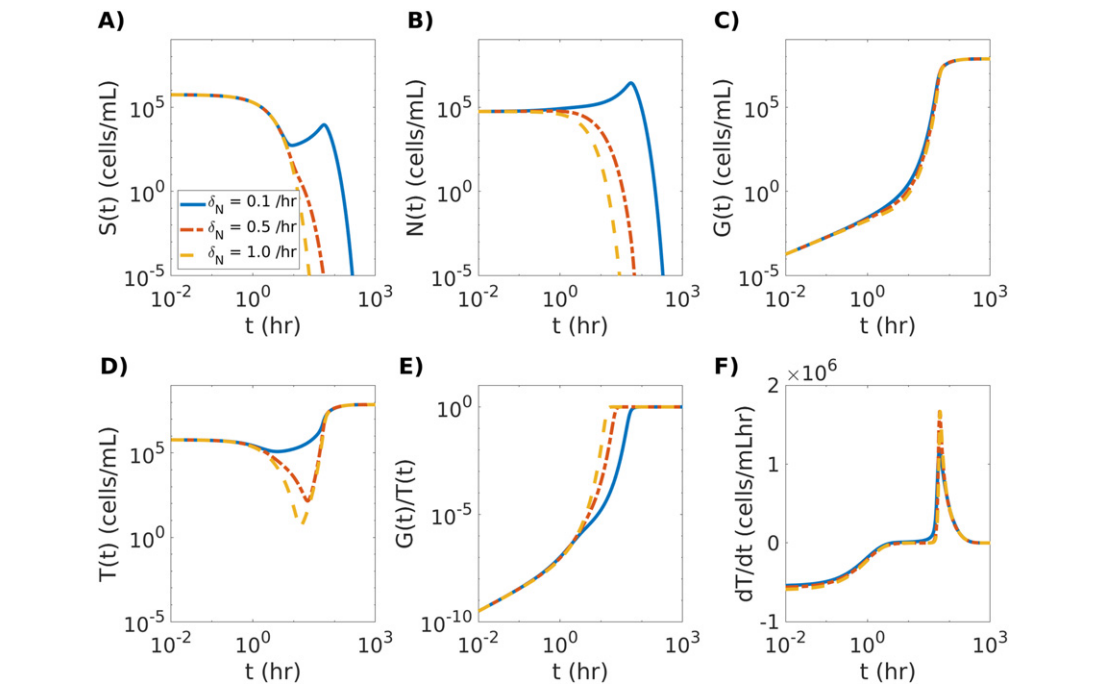

Figure D1. Growth of the genetically resistant subpopulation is hindered by the growth of the non-genetically resistant subpopulation with a low birth rate in cidal drug environment. (A) The growth curve of the drug susceptible (S) subpopulation. (B) The growth curve of the non-genetically drug resistant (N) subpopulation. (C) The growth curve of the genetically drug resistant (G) subpopulation. (D) The growth curve of the total population (T). (E) The fraction of $G(t)$ in the total population T. (F) The rate of change in the size of T ($\mathrm{d}T/\mathrm{d}t$) as a function of time. Each coloured line represents a different numerical simulation corresponding to the death rates of N shown in the legend in (A), with the solid blue line representing the highest level of N fitness (death rate of 0.1 h^{-1}), the red dash-dotted line an intermediate level of N fitness (death rate of 0.5 h^{-1}), and the yellow dashed line the lowest level N fitness (death rate of 1.0 h^{-1}) relative to the fitness of G (unaffected by the drug) during cidal drug treatment. S was given a death rate of $\delta_S = 1.0\ \mathrm{h}^{-1}$ for these simulations, and the birth rate of G was set to $k_N = 0.3466\ \mathrm{h}^{-1}$.

S population significantly less fit relative to N and G subpopulations regardless of the cidal drug strength.

Appendix D. Cidal drug simulations with low N birth rate

Here we consider a cidal drug scenario where N has a low birth rate relative to G by setting $k_N = 0.1733\ \mathrm{h}^{-1}$, while k_G remained at 0.3466 h^{-1}. Subpopulation trajectories, the fraction of genetically drug resistant cells in the population G/T, and the population rate of change $\mathrm{d}T/\mathrm{d}t$ for this case are shown in figure D1. A fixation time heat map for this case is shown in figure D2. The qualitative trends and conclusions made in the main text hold for this scenario.

Appendix E. Partially drug-susceptible genetic mutant

Figure E1 shows a cidal drug case where G is assigned a death rate of $\delta_G = 0.5\ \mathrm{h}^{-1}$ and hence is not fully resistant to the drug. The time series show three

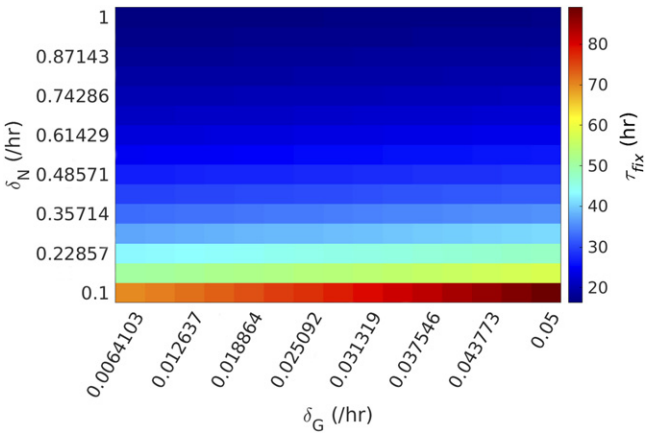

Figure D2. Drug resistance of the non-genetic subpopulation slows the development of the genetically drug resistant subpopulation in a cidal drug environment with N having a low birth rate relative to G ($k_N = 0.1733\ \mathrm{h}^{-1}$). Heat map shows the effect of the death rates of the non-genetically resistant (δ_N) and genetically resistant (δ_G) subpopulations on the fixation time (τ_{fix}) of G under cidal drug treatment. Each bin corresponds to a simulation for a combination of δ_N and δ_G parameter values. The colour map show the fixation time in hours.

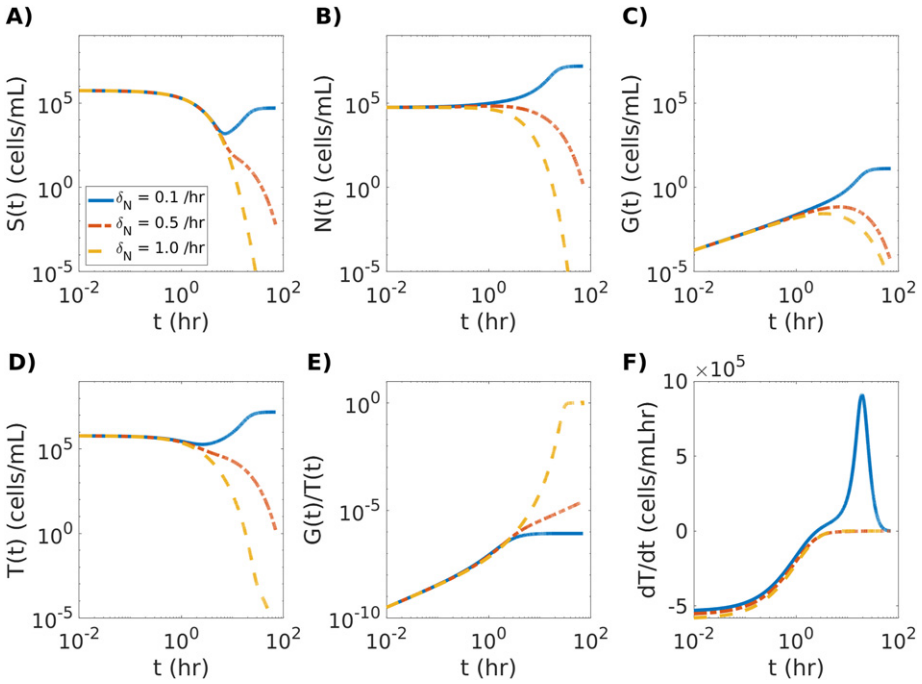

Figure E1. Partially resistant genetic mutation results in either total population extinction or non-zero steady-state population size during cidal drug treatment ($\delta_G = 0.5\ \mathrm{h}^{-1}$). (A) The growth curve of the drug susceptible (S) subpopulation. (B) The growth curve of the non-genetically drug resistant (N) subpopulation. (C) The growth curve of the genetically partially drug resistant (G) subpopulation. (D) The growth curve of the total population (T). (E) The fraction of $G(t)$ in T. (F) The rate of change in the size of T ($\mathrm{d}T/\mathrm{d}t$) as a function of time. Each coloured line represents a different numerical simulation using the death rate values shown in the legend in (A), with the solid blue line representing the highest level of N fitness ($\delta_N = 0.1\ \mathrm{h}^{-1}$), the red dash-dotted line an intermediate level of N fitness ($\delta_N = 0.5\ \mathrm{h}^{-1}$), and the yellow dashed line the lowest level of N fitness ($\delta_N = 1.0\ \mathrm{h}^{-1}$) relative to the intermediate fitness level of G ($\delta_G = 0.5\ \mathrm{h}^{-1}$).

different cases. The first case is where N has a relatively high-fitness death rate, resulting in the total population moving toward a non-zero steady state over time (solid blue lines in figure E1). The second case captures a scenario where N and G have the same intermediate fitness death rate, resulting in extinction of the total population (dash-dotted red lines in figure E1). The last case shows a situation where N has a low fitness death rate that is greater than the death rate of G, which also results in total population extinction (dashed yellow lines in figure E1). Consistent with our main results, this case shows that the fitness of N hinders the evolution of G, even when G is partly susceptible to the drug.

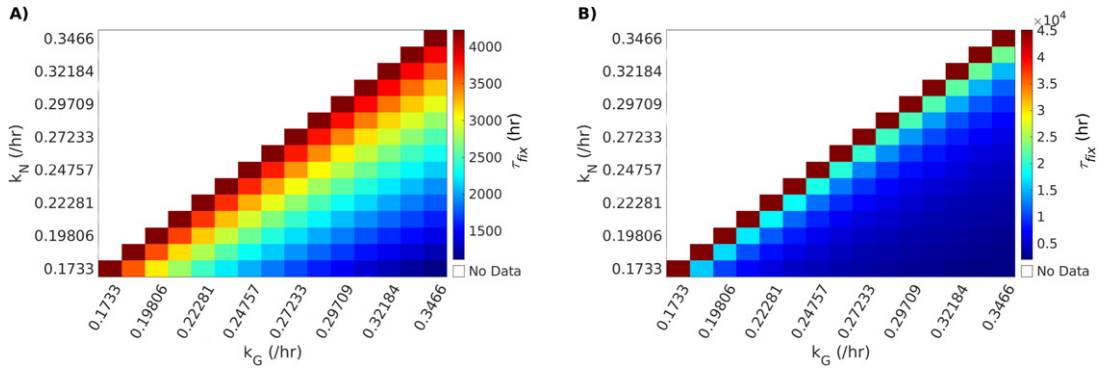

Figure F1. Genetic fixation results in the static drug environment for different values of switching rate $r_{N,S}$. (A) $r_{N,S} = 0.001$ h^{-1}. (B) $r_{N,S} = 0.1$ h^{-1}.

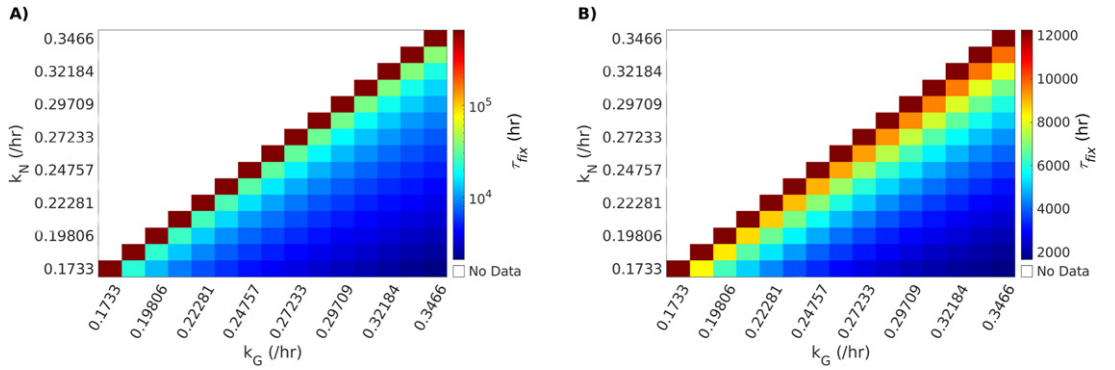

Figure F2. Genetic fixation results in the static drug environment for different values of switching rate $r_{S,N}$. (A) $r_{S,N} = 0.0001$ h^{-1}. Due to the large range of values (ranging from 2080 h to over 10^6 hr) this color map was plotted on a log scale. (B) $r_{S,N} = 0.01$ h^{-1}.

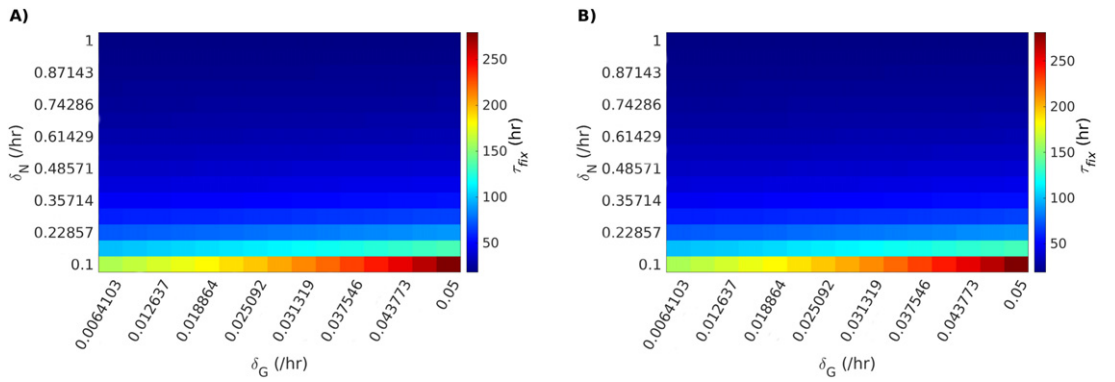

Figure F3. Genetic fixation results in the cidal drug environment for different values of switching rate $r_{N,S}$. (A) $r_{N,S} = 0.001$ h^{-1}. (B) $r_{N,S} = 0.1$ h^{-1}.

Appendix F. Parameter scans of switching and mutation rates

To further test the robustness of our main findings, we performed order-of-magnitude parameter scans of the switching rates $r_{N,S}$ and $r_{S,N}$ (figures F1–F4), as well as the mutation rate $r_{G,N}$ (figures F5 and F6), for the static and cidal drug scenarios.

Specifically, when the switching rate from S to N ($r_{N,S}$) was decreased by an order of magnitude it reduced the timescale (i.e., slightly decreased the lower bound of τ_{fix} and drastically decreased the upper bound of τ_{fix}) over which G fixed in the population (figure F1(A)); (2) when the switching rate from N to S ($r_{S,N}$) was decreased by an order of magnitude it increased the timescale (i.e., slightly decreased the lower bound of τ_{fix} and drastically increased the upper bound of τ_{fix}) over which G evolved in the population (figure F2(A)); and (3) when the switching rate from N to S ($r_{S,N}$) was increased by an order

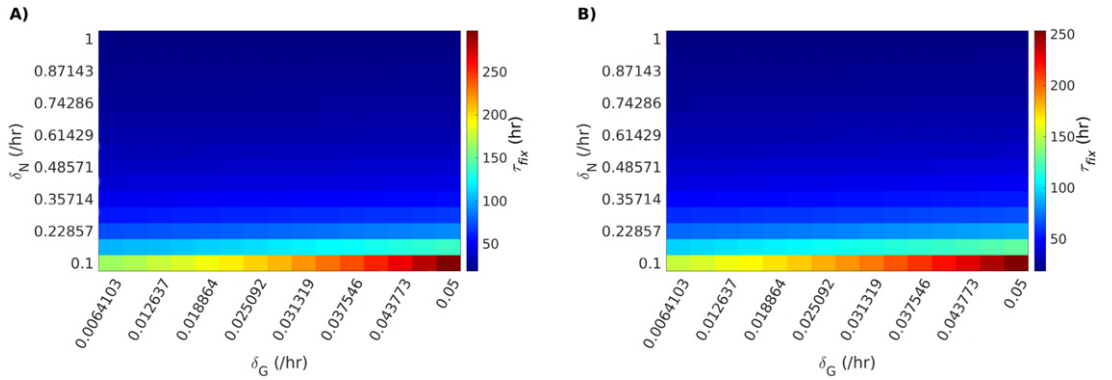

Figure F4. Genetic fixation results in the cidal drug environment for different values of switching rate $r_{S,N}$. (A) $r_{S,N} = 0.0001$ h^{-1}. (B) $r_{S,N} = 0.01$ h^{-1}.

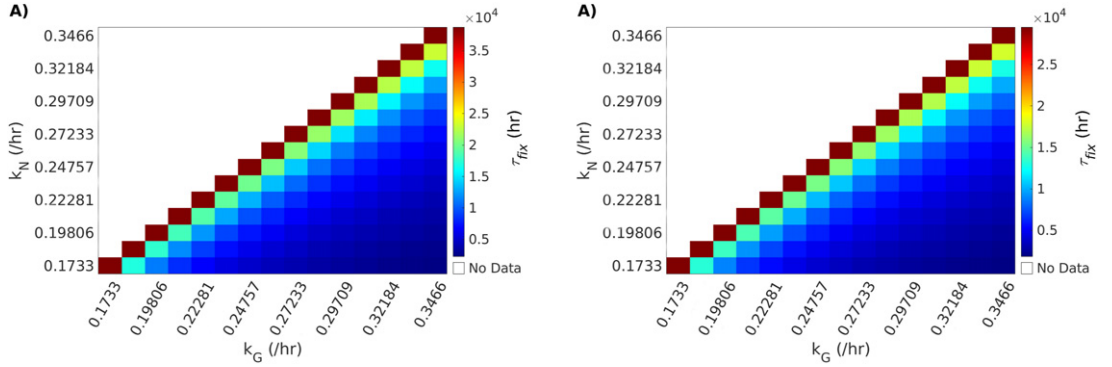

Figure F5. Genetic fixation results in the static drug environment for different values of mutation rate $r_{G,N}$. (A) $r_{G,N} = 10^{-7}/4$ h (B) $r_{G,N} = 10^{-6}/2$ h.

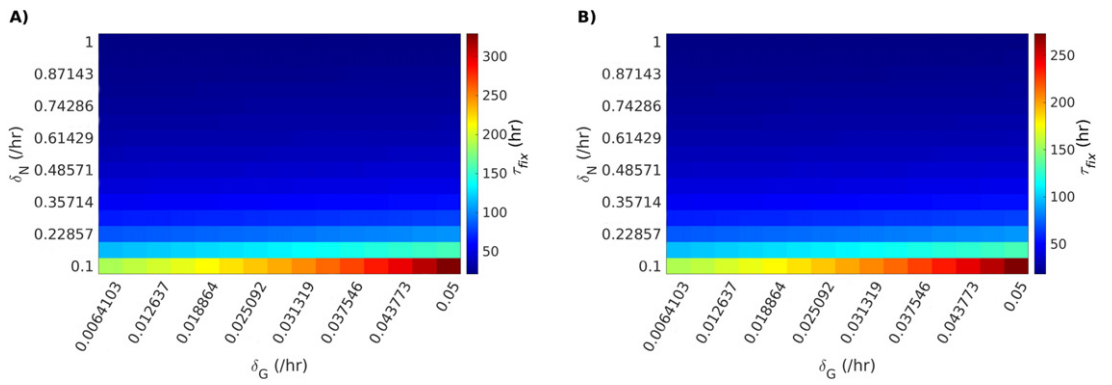

Figure F6. Genetic fixation results in the cidal drug environment for different values of mutation rate $r_{G,N}$. (A) $r_{G,N} = 10^{-7}/4$ h (B) $r_{G,N} = 10^{-6}/2$ h.

of magnitude, it decreased the timescale (i.e., slightly decreased the lower bound of τ_{fix} and drastically decreased the upper bound of τ_{fix}) over which G fixed in the population (figure F2(B)). One might expect that any change that leads to an increase in N would also increase G (because N mutates to G) and therefore would decrease the fixation of time of G, however, this was not the case and the evolution of G depended on the interactions between the competing subpopulations.

There were no important differences were observed for parameter scans of the N to G mutation rate (figures F5 and F6).

Overall, these results demonstrate that the conclusions made in the main text hold for a wide range of parameters, though changing the switching rates

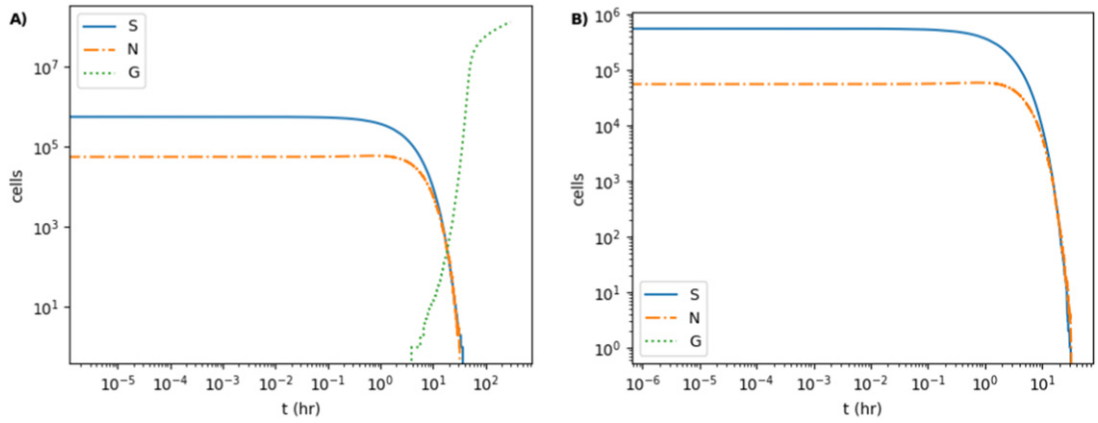

Figure G1. Cell population survival and extinction during cidal drug treatment. (A) A representative population non-extinction case where G appears before S and N go extinct. (B) A representative population extinction case where S and N go extinct before G appears in the population.

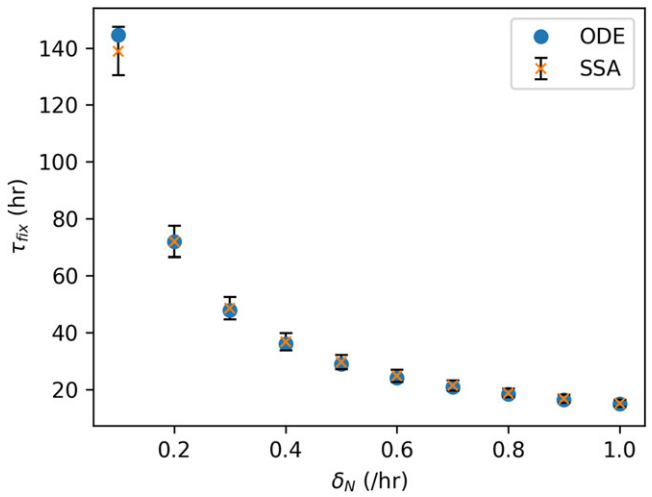

Figure H1. Genetic subpopulation G fixation time comparison for deterministic ODE and SSA simulations with a pre-existing mutation ($G_i = 1$). Genetic fixation time τ_{fix} is shown as a function of non-genetic subpopulation N fitness (δ_N) in the cidal drug environment. The death rate of the susceptible population S was set to $\delta_S = 1.0\ \text{h}^{-1}$ and the birth rates of N and G were set to $k_N = k_G = 0.3466\ \text{h}^{-1}$ for these simulations. Error bars on the SSA results show the standard deviation.

qualitatively affects the evolution of drug-resistant mutants in a way that is not entirely obvious and that depends on the underlying population dynamics.

Appendix G. Survival and extinction scenarios

Representative survival and extinction trajectories from the stochastic simulations are shown in figure G1. Figure G1(A) shows a case where the cell population survives cidal drug treatment due to G emerging before S and N go extinct. G subsequently takes over the population in this scenario. In contrast, figure G1(B) shows a case where the cell population goes extinct due to S and N reaching zero cells before G appears.

Appendix H. Pre-existing mutation for stochastic simulations

To show that the discrepancies seen in figure 7 were due to differences between the modeling approaches, i.e., SSA models extinction due to stochasticity in τ_{app}, simulations using a pre-existing mutation ($G_i = 1$) were made. Figure H1 shows the comparison of genetic fixation times calculated using simulations from the deterministic ODE and SSA modeling approaches, similar to figure 7 in the main text. As seen, removing the possibility of extinction by removing the stochastic nature of the first appearance time of G results in the SSA results converging to those found using the deterministic ODE model.

Appendix I. Varying initial population sizes

Starting the deterministic simulations with a low or high initial population size ($T_i \approx 10^3$ or $T_i \approx 10^8$) or with varying amounts of initial non-genetically resistant cells (N_i making up 1%–20% of T_i) were found to have little effect on the fixation time of the genetically resistant population, as the population dynamics in these cases quickly converged to similar trajectories regardless of their initial population sizes. For the stochastic simulations the initial population size was found to aid survival, with high initial populations surviving the drug for longer amounts of time and hence providing more time for the mutant population to emerge, as expected, but the fixation times of the genetically resistant population were once again not strongly affected by varying T_i or N_i.

ORCID iDs

Joshua D Guthrie https://orcid.org/0000-0002-5160-5363
Daniel A Charlebois https://orcid.org/0000-0001-7426-1789

References

[1] O'Neill J 2016 The review on antimicrobial resistance *Tackling Drug-Resistant Infections Globally: Final Report and Recommendations* (London: Wellcome Trust)
[2] Salmond G P and Welch M 2008 Antibiotic resistance: adaptive evolution *Lancet* **372** S97–103
[3] Fraser D and Kaern M 2009 A chance at survival: gene expression noise and phenotypic diversification strategies *Mol. Microbiol.* **71** 1333–40
[4] Levin B R and Rozen D E 2006 Non-inherited antibiotic resistance *Nat. Rev. Microbiol.* **4** 556–62
[5] Farquhar K S, Rasouli Koohi S and Charlebois D A 2021 Does transcriptional heterogeneity facilitate the development of genetic drug resistance? *BioEssays* **43** 2100043
[6] Charlebois D A, Abdennur N and Kaern M 2011 Gene expression noise facilitates adaptation and drug resistance independently of mutation *Phys. Rev. Lett.* **107** 218101
[7] Munsky B, Neuert G and van Oudenaarden A 2012 Using gene expression noise to understand gene regulation *Science* **336** 183–7
[8] Samoilov M S, Price G and Arkin A P 2006 From fluctuations to phenotypes: the physiology of noise *Nat. Rev. Genet.* **2006** re17
[9] Blake W J, Balázsi G, Kohanski M A, Isaacs F J, Murphy K F, Kuang Y, Cantor C R, Walt D R and Collins J J 2006 Phenotypic consequences of promoter-mediated transcriptional noise *Mol. Cell* **24** 853–65
[10] Brock A, Chang H and Huang S 2009 Non-genetic heterogeneity—a mutation-independent driving force for the somatic evolution of tumours *Nat. Rev. Genet.* **10** 336–42
[11] Kærn M, Elston T C, Blake W J and Collins J J 2005 Stochasticity in gene expression: from theories to phenotypes *Nat. Rev. Genet.* **6** 451–64
[12] Berman J and Krysan D J 2020 Drug resistance and tolerance in fungi *Nat. Rev. Microbiol.* **18** 319–31
[13] Gefen O and Balaban N Q 2009 The importance of being persistent: heterogeneity of bacterial populations under antibiotic stress *FEMS Microbiol. Rev.* **33** 704–17
[14] Wakamoto Y, Dhar N, Chait R, Schneider K, Signorino-Gelo F, Leibler S and McKinney J D 2013 Dynamic persistence of antibiotic-stressed mycobacteria *Science* **339** 91–5
[15] Vallette F M, Olivier C, Lezot F, Oliver L, Cochonneau D, Lalier L, Cartron P-F and Heymann D 2019 Dormant, quiescent, tolerant and persister cells: four synonyms for the same target in cancer *Biochem. Pharmacol.* **162** 169–76
[16] Levin-Reisman I, Ronin I, Gefen O, Braniss I, Shoresh N and Balaban N Q 2017 Antibiotic tolerance facilitates the evolution of resistance *Science* **355** 826–30
[17] Charlebois D A, Balazsi G and Kaern M 2014 Coherent feedforward transcriptional regulatory motifs enhance drug resistance *Phys. Rev.* E **89** 052708
[18] Camellato B, Roney I J, Azizi A, Charlebois D and Kaern M 2019 Engineered gene networks enable non-genetic drug resistance and enhanced cellular robustness *Eng. Biol.* **3** 72–9
[19] Farquhar K S, Charlebois D A, Szenk M, Cohen J, Nevozhay D and Balázsi G 2019 Role of network-mediated stochasticity in mammalian drug resistance *Nat. Commun.* **10** 2766
[20] Bar-Even A, Paulsson J, Maheshri N, Carmi M, O'Shea E, Pilpel Y and Barkai N 2006 Noise in protein expression scales with natural protein abundance *Nat. Genet.* **38** 636–43
[21] Newman J R S, Ghaemmaghami S, Ihmels J, Breslow D K, Noble M, DeRisi J L and Weissman J S 2006 Single-cell proteomic analysis of *S. cerevisiae* reveals the architecture of biological noise *Nature* **441** 840–6
[22] Liu J, François J-M and Capp J-P 2019 Gene expression noise produces cell-to-cell heterogeneity in eukaryotic homologous recombination rate *Front. Genet.* **10** 475
[23] Uphoff S, Lord N D, Okumus B, Potvin-Trottier L, Sherratt D J and Paulsson J 2016 Stochastic activation of a DNA damage response causes cell-to-cell mutation rate variation *Science* **351** 1094–7
[24] Bódi Z *et al* 2017 Phenotypic heterogeneity promotes adaptive evolution *PLoS Biol.* **15** e2000644
[25] Zhang Z, Qian W and Zhang J 2009 Positive selection for elevated gene expression noise in yeast *Mol. Syst. Biol.* **5** 299
[26] You S-T and Leu J-Y 2020 Making sense of noise *Evolutionary Biology—A Transdisciplinary Approach* ed P Pontarotti (Cham: Springer) pp 379–91
[27] Freddolino P L, Yang J, Momen-Roknabadi A and Tavazoie S 2018 Stochastic tuning of gene expression enables cellular adaptation in the absence of pre-existing regulatory circuitry *eLife* **7** e31867
[28] Ghalambor C K, Hoke K L, Ruell E W, Fischer E K, Reznick D N and Hughes K A 2015 Non-adaptive plasticity potentiates rapid adaptive evolution of gene expression in nature *Nature* **525** 372–5
[29] van Rhijn N and Bromley M 2021 The consequences of our changing environment on life threatening and debilitating fungal diseases in humans *J. Fungi* **7** 367
[30] Sears D and Schwartz B S 2017 *Candida auris*: an emerging multidrug-resistant pathogen *Int. J. Infect. Dis.* **63** 95–8
[31] Farquhar K S, Flohr H and Charlebois D A 2020 Advancing antimicrobial resistance research through quantitative modeling and synthetic biology *Front. Bioeng. Biotechnol.* **8** 583415
[32] Nevozhay D, Adams R M, Itallie E V, Bennett M R and Balazsi G 2012 Mapping the environmental fitness landscape of a synthetic gene circuit *PLoS Comput. Biol.* **8** e1002480
[33] González C, Ray J C J, Manhart M, Adams R M, Nevozhay D, Morozov A V and Balázsi G 2015 Stress-response balance drives the evolution of a network module and its host genome *Mol. Syst. Biol.* **11** 827

[34] Baishya J and Wakeman C A 2019 Selective pressures during chronic infection drive microbial competition and cooperation *npj Biofilms Microbiome* **5** 16
[35] Baishya J, Bisht K, Rimbey J N, Yihunie K D, Islam S, Al Mahmud H, Waller J E and Wakeman C A 2021 The impact of intraspecies and interspecies bacterial interactions on disease outcome *Pathogens* **10** 96
[36] Hibbing M E, Fuqua C, Parsek M R and Peterson S B 2010 Bacterial competition: surviving and thriving in the microbial jungle *Nat. Rev. Microbiol.* **8** 15–25
[37] Charlebois D A and Balázsi G 2019 Modeling cell population dynamics *Silico Biol.* **13** 21–39
[38] Ackermann M 2015 A functional perspective on phenotypic heterogeneity in microorganisms *Nat. Rev. Microbiol.* **13** 497–508
[39] Bell G and MacLean C 2018 The search for 'evolution-proof' antibiotics *Trends Microbiol.* **26** 471–83
[40] Fridman O, Goldberg A, Ronin I, Shoresh N and Balaban N Q 2014 Optimization of lag time underlies antibiotic tolerance in evolved bacterial populations *Nature* **513** 418–21
[41] (2021) MATLAB Version 9.10.0 (R2021a) (Natick, Massachusetts: The MathWorks Inc.)
[42] Klironomos F D, Berg J and Collins S 2013 How epigenetic mutations can affect genetic evolution: model and mechanism *BioEssays* **35** 571–8
[43] Gillespie D T 1976 A general method for numerically simulating the stochastic time evolution of coupled chemical reactions *J. Comput. Phys.* **22** 403–34
[44] Gillespie D T 1977 Exact stochastic simulation of coupled chemical reactions *J. Phys. Chem.* **81** 2340–61
[45] Longo V D, Shadel G S, Kaeberlein M and Kennedy B 2012 Replicative and chronological aging in *Saccharomyces cerevisiae Cell Metab.* **16** 18–31
[46] Ramia N E, Mangavel C, Gaiani C, Muller-Gueudin A, Taha S, Revol-Junelles A-M and Borges F 2020 Nested structure of intraspecific competition network in *Carnobacterium maltaromaticum Sci. Rep.* **10** 7335
[47] Karr J R, Sanghvi J C, Macklin D N, Gutschow M V, Jacobs J M, Bolival B Jr, Assad-Garcia N, Glass J I and Covert M W 2012 A whole-cell computational model predicts phenotype from genotype *Cell* **150** 389–401
[48] Ribeiro A 2008 Dynamics and evolution of stochastic bistable gene networks with sensing in fluctuating environments *Phys. Rev.* E **78** 061902
[49] Weiße A Y, Oyarzúnc D A, Danos V and Swain P S 2015 Mechanistic links between cellular trade-offs, gene expression, and growth *Proc. Natl. Acad. Sci. USA* **112** E1038
[50] Jo M C, Liu W, Gu L, Dang W and Qin L 2015 High-throughput analysis of yeast replicative aging using a microfluidic system *Proc. Natl Acad. Sci. USA* **112** 9364–9
[51] Charlebois D A, Hauser K, Marshall S and Balazsi G 2018 Multiscale effects of heating and cooling on genes and gene networks *Proc. Natl Acad. Sci. USA* **115** E10797
[52] Acar M, Mettetal J T and Van Oudenaarden A 2008 Stochastic switching as a survival strategy in fluctuating environments *Nat. Genet.* **40** 471–5
[53] Beaumont H J E, Gallie J, Kost C, Ferguson G C and Rainey P B 2009 Experimental evolution of bet hedging *Nature* **462** 90–3
[54] Singh A and Hespanha J P 2010 Stochastic hybrid systems for studying biochemical processes *Phil. Trans. R. Soc.* A **368** 4995–5011
[55] Ghusinga K R, Dennehy J J and Singh A 2017 First-passage time approach to controlling noise in the timing of intracellular events *Proc. Natl Acad. Sci. USA* **114** 693–8
[56] Baym M, Stone L K and Kishony R 2016 Multidrug evolutionary strategies to reverse antibiotic resistance *Science* **351** aad3292
[57] Dar R D, Hosmane N N, Arkin M R, Siliciano R F and Weinberger L S 2014 Screening for noise in gene expression identifies drug synergies *Science* **344** 1392–6
[58] Melnyk A H, Wong A and Kassen R 2015 The fitness costs of antibiotic resistance mutations *Evol. Appl.* **8** 273–83
[59] Alon U 2020 *An Introduction to Systems Biology: Design Principles of Biological Circuits* 2nd edn (Boca Raton, FL: CRC Press)
[60] Charlebois D A, Diao J, Nevozhay D and Balázsi G 2018 Negative regulation gene circuits for efflux pump control *Methods Mol. Biol.* **1772** 25–43